TISSUE ENGINEERING: Part A
Volume 20, Numbers 19 and 20, 2014

DOI: 10.1089/ten.tea.2013.0687

Tunable Engineered Skin Mechanics via Coaxial Electrospun Fiber Core Diameter

Britani Nicole Blackstone, MS,[1,2] Jason William Drexler, MS,[3] and Heather Megan Powell, PhD[1–4]

Autologous engineered skin (ES) offers promise as a treatment for massive full thickness burns. Unfortunately, ES is orders of magnitude weaker than normal human skin causing it to be difficult to apply surgically and subject to damage by mechanical shear in the early phases of engraftment. In addition, no manufacturing strategy has been developed to tune ES biomechanics to approximate the native biomechanics at different anatomic locations. To enhance and tune ES biomechanics, a coaxial (CoA) electrospun scaffold platform was developed from polycaprolactone (PCL, core) and gelatin (shell). The ability of the coaxial fiber core diameter to control both scaffold and tissue mechanics was investigated along with the ability of the gelatin shell to facilitate cell adhesion and skin development compared to pure gelatin, pure PCL, and a gelatin-PCL blended fiber scaffold. CoA ES exhibited increased cellular adhesion and metabolism versus PCL alone or gelatin-PCL blend and promoted the development of well stratified skin with a dense dermal layer and a differentiated epidermal layer. Biomechanics of the scaffold and ES scaled linearly with core diameter suggesting that this scaffold platform could be utilized to tailor ES mechanics for their intended grafting site and reduce graft damage *in vitro* and *in vivo*.

Introduction

Burn injuries are all too prevalent in the U.S. with ~450,000 burn injuries and 3400 burn and fire related mortalities reported in the U.S. in 2011 alone.[1] Times of military conflict see an increase in incidence of burn injuries and 5–20% of military casualties are attributed to such injuries.[2] Patient outcomes have improved in the past few decades due to advances in areas of burn care such as infection control.[3–9] However, the standard treatment for full-thickness burns, split-thickness autograft (AG), is deficient for massive burn injuries. In large burns, sparse availability of uninjured skin prevents rapid closure of the wound resulting in increased scar tissue formation or mortality. Tissue engineered skin (ES) offers promise as an adjuvant burn therapy when autograft is not readily available and numerous tissue ES replacements have been created.[10–20] Autologous ES provides several advantages over conventional therapy including reduction in donor site area required to permanently close wounds. For example, conventional grafting expands donor skin by about 1:4. In contrast, ES have been shown to heal ~60 times the area of the initial skin biopsy collected from the patient.[20] Thus, the potential clinical impacts of ES are substantial. Unfortunately, autologous ES does not completely mimic the physical and biological properties of native human skin.

Current collagen-based models of ES are greater than three orders of magnitude weaker than normal human skin,[18,21] resulting in increased susceptibility to damage by mechanical shear during fabrication and early engraftment, difficulty during surgical application, and suboptimal biomechanical function when compared with native tissue. Methods to improve ES mechanics would not only aid in the manufacturing process but may provide superior functional outcome for patients. Human skin exhibits significantly different mechanical properties based on anatomic location and the ability to control ES mechanics would allow engineers to approximate the mechanics of ES to the graft site. For example, forehead skin is stiffer, thicker, and less elastic than skin at the ventral forearm[22] and ten times more rigid than cheek skin.[23] Skin at the palms and feet exhibit significantly less elasticity than other locations,[24] skin at the abdomen and postauricular has been reported to display a six-fold increase in immediate distension and retraction compared with the ankle and a greater than 10-fold increase compared with the palm.[24] Additionally, dorsal finger skin is two to four times harder than ventral fingers, forearms, face, chest, and lower legs.[25] Thus, ability to tailor mechanical properties of ES would allow for the selection of the properties that better suit the target area and patient.

Mechanical testing of the epidermis and dermis in native human skin and in ES showed dramatic differences in

[1]Department of Biomedical Engineering, [2]NSEC Center for Affordable Polymeric Biomedical Devices, and [3]Department of Materials Science and Engineering, The Ohio State University, Columbus, Ohio.
[4]Research Department, Shriners Hospitals for Children, Cincinnati, Ohio.

properties between the two tissues. The greatest disparity was measured in the dermal component where the elastic modulus of the dermis in ES (22.3–33.9 kPa)[26] was three orders of magnitude less stiff than reported values for native human dermis (15.6–60.8 MPa).[27–30] In contrast, the average modulus of the epidermis in normal human skin (5.0 ± 1.7 MPa) was approximately double that of ES (2.4 ± 1.1 MPa)[31] suggesting that the dermis/scaffold is the most suitable target for biomechanical enhancement. Numerous prior studies have been completed that aim to improve ES mechanics via scaffold properties.[18] Chemical cross-linking[32–35] and polymer-blends[18,36–39] were investigated and show that the maturation and viability of the ES were critical to overall mechanical function and ES mechanics was not solely dependent on scaffold mechanics. Thus, a scaffold platform that can be mechanically tuned without altering cellular function and tissue development is needed to enhance and tailor the mechanics of ES.

Coaxial (CoA or core-shell) electrospinning offers the ability to alter the mechanical properties of the scaffold while maintaining a continuous biologically active shell with which cells interact given surface chemistry.[40,41] The goal of this study was to use coaxial electrospinning to develop a cell-scaffold system capable of providing ES with tunable biomechanics. To achieve this goal, polycaprolactone (PCL)-gelatin coaxial electrospun scaffolds were investigated as a potential scaffold platform for skin manufacturing. While gelatin is known to offer biocompatibility, its fairly weak mechanical properties often require reinforcement in the application of wound healing.[42–44] Conversely, PCL offers significant scaffold strength, while its hydrophobicity has been shown to decrease cell viability.[45,46] As a result, gelatin and PCL have previously been blended in an effort to compensate for their shortcomings.[47–50] However, even slight additions (greater than 1%) of PCL to a biopolymer affected ES development and, as a result, no significant increase in ES strength was observed,[18] most likely due to cellular interactions with PCL. In this study, the effect of core diameter of coaxial fibers (PCL core, gelatin shell) on cellular adhesion, scaffold, and ES mechanical properties and ES morphogenesis was investigated and compared with electrospun gelatin, PCL, and gelatin-PCL blended scaffolds.

Materials and Methods

Scaffold fabrication

Electrospinning solutions were made as described previously.[40] Briefly, gelatin (Sigma-Aldrich) or polycaprolactone (PCL; Sigma-Aldrich; $M_n = 42{,}500$) were dissolved in 1,1,1,3,3,3-hexafluoro-2-propanol (HFP; Sigma-Aldrich). A total of seven scaffolds were made including four coaxial, pure gelatin, pure PCL, and a 1:1 PCL-gelatin blend. Coaxial scaffolds (CoA-S, CoA-M, CoA-L, and CoA-XL) were all spun with a 12 wt/vol.% solution of gelatin in HFP for the shell of the fiber and the PCL core concentrations were varied from 8 to 12 w/v% (Table 1). The flow rate of the gelatin shell was 4 mL/h for all coaxial scaffolds and the flow rate of the core ranged from 1 to 2 mL/h (Table 1). Coaxial scaffolds were electrospun at a potential of 15–20 kV onto 9×9 cm aluminum foil covered grounding plates. The three control solutions in HFP, PCL (14 w/v%), gelatin (12 w/v%), and a blend of the two (Blend, 12 w/v%), were electrospun at flow rates of 15, 12, and 12 mL/h respectively at a voltage of 26, 23, and 19 kV respectively onto an 8.5 cm^2 grounded plate at a distance of 20 cm. Prior to use, all scaffolds were removed from the aluminum foil, and cross-linked in a 7 mM solution of ethanol and N-(3-dimethylaminopropyl)-N′-ethylcarbodiimide hydrochloride (EDC; Sigma-Aldrich Co.) to stabilize the gelatin. Scaffolds were soaked in 70% ethanol to disinfect and to render the PCL scaffolds wettable. Following disinfection, scaffolds were rinsed in sterile HEPES buffered saline with five exchanges of fluid and then soaked in culture medium for a minimum of 3 h prior to use.

Table 1. Concentrations and Feed Rates for Coaxial Scaffolds

Scaffold name	*PCL core solution concentration (wt./vol.%)*	*PCL core solution feed rate (mL/h)*
CoA-S	8	1
CoA-M	12	1
CoA-L	10	2
CoA-XL	12	2

PCL, polycaprolactone.

Fourier transform infrared spectroscopy

Attenuated Total Reflectance-Fourier Transform Infrared (ATR-FTIR) spectroscopy of all scaffold types was obtained on a Nicolet Nexus 670 benchtop FTIR spectrometer and a Continuum microIR microscope (Thermo Scientific), using a germanium crystal. IR spectra were obtained over a wavenumber range of 600–4000 cm^{-1} at a resolution of 8 cm^{-1}. Scaffolds were imaged following a 24 h drying period in a vacuum oven held at 40°C. Scaffold compositions were assessed qualitatively by comparing absorbance peaks associated with electrospun PCL (1724 cm^{-1} carbonyl, 1240 cm^{-1} asymmetric COC stretching, 1190 cm^{-1} OC-O stretching, 1170 cm^{-1} symmetric COC stretching, and 1157 cm^{-1} C-O and C-C stretching in the amorphous phase) and gelatin (amide bonds at 1650 and 1540 cm^{-1}). Representative absorbance versus wavenumber^{-1} peaks were plotted for each scaffold type. Data are shown only from 1800 to 1000 cm^{-1} to provide more detail for visual comparison.

Cell culture

Human epidermal keratinocytes (CK) and dermal fibroblasts (CF) were simultaneously isolated from surgical discard tissue. Adult female breast skin for culture of human cells was obtained under a protocol approved by the Ohio State University Institutional Review Board. All CFs were cultured in DME (Invitrogen) supplemented with 4% fetal bovine serum (Invitrogen), 5 μg/mL bovine insulin (Sigma), 10 ng/mL epidermal growth factor (EGF; PeproTech), 0.5 μg/mL hydrocortisone (Sigma), and 0.1 mM L-ascorbic acid-2-phosphate (Sigma). CK were cultured in 153 (Sigma) supplemented with 5 μg/mL bovine insulin (Sigma), 1 ng/mL EGF, 0.5 μg/mL hydrocortisone, and 0.2 vol% bovine pituitary extract (Gemini BioProducts). Cells were isolated and cryopreserved at passage 0 (primary culture) and with passage 1 providing a stock of cells for the ES.

Cell adhesion

Relative strength of human dermal fibroblast (CF) and human epidermal keratinocyte (CK) adhesion to the coaxial fibers (CoA-S and CoA-XL) was compared with Gelatin, PCL, and Blend fibers using a parallel-plate assay as previously described.[51] Of the coaxial scaffolds, only CoA-S and CoA-XL were tested as the goal was to determine whether the gelatin shell improved adhesion versus PCL and the Blend and whether the thickness of the shell altered strength of adhesion. Fibroblasts and keratinocytes were stained with CellTracker™ Green CMFDA (Invitrogen) according to manufacturer's protocol, harvested, and inoculated at 15,000 cells/cm^2 onto scaffolds electrospun onto microscope slides. Samples ($n=4$ per cell line and scaffold type) were incubated in a humidified chamber at 37°C with 5% CO_2 for 90 min, loaded into a parallel-plate device, and subjected to a shear stress of 500 dynes/cm^2 for 5 min. Strength of adhesion was quantified by imaging slides using fluorescent microscopy (Nikon Eclipse LV150) before and after shear stress exposure ($n=7$), with average percent cells remaining ± standard error of the mean being reported. All images were captured along the center line of the device and 10 mm inside of each port where the fluid velocity and surface shear profiles were previously determined to be uniform.[51]

Formation of ES

Cross-linked scaffolds (9 × 9 cm) were seeded with human primary dermal fibroblasts (CF) at a density of 5×10^5 cells/cm^2 and epidermal keratinocytes (CK) at a density of 1.0×10^6 cells/cm^2. After inoculation of CF, the cell-scaffold construct was incubated, floating in a 150 mm diameter tissue culture dish (BD Falcon) at 37°C and 5% CO_2 in DME supplemented with 1 mM strontium chloride (Sigma), 2 μg/mL linoleic acid (Sigma), 5 μg/mL bovine insulin, 20 pM triiodothyronine (Sigma), 0.5 μg/mL hydrocortisone (Simga), 0.1 mM ascorbic acid-3-phosphate, 0.76 nM progesterone (Sigma), and 10 ng/mL EGF[52] for 1 day followed by inoculation of CK. One day after inoculation of CK, the tissue was placed on a perforated stainless steel frame with a cotton sheet in between the frame and tissue. Progesterone and EGF were removed from culture medium 3 days after CK inoculation. The ES was then cultured for up to 21 days at the air–liquid interface by placing the ES on a perforated stainless steel lifting frame, covered with a thin, permeable cotton pad (Whatman, GE Healthcare) to aid in wicking medium to the dermis.

Tensile testing

Tensile testing was used to quantify the mechanical properties of acellular scaffolds and ES ($n=6$ for each condition). Acellular scaffolds were prepared for mechanical testing by cross-linking each scaffold in a 7 mM solution of N-(3-dimethylaminopropyl)-N′-ethylcarbodiimide hydrochloride (EDC; Sigma-Aldrich Co.) and 100 mL of pure ethanol for 24 h, hydrated using HEPES buffered saline (HBS), and punched into dog-bone-shaped tensile specimens with a width of 4 mm and gauge length of 20 mm. ES was cultured for 19 days prior to tensile testing. The samples were secured in the grips of a tensile tester (TestResources 100R) and loaded until failure at a rate of 2 mm/s to prevent scaffold dehydration. Data from samples that did not break within the gauge length were discarded. Ultimate tensile strength (UTS) and stiffness were measured and reported as mean ± standard deviation.

Cellular metabolism

A modified MTT assay was performed to quantify the cellular metabolic activity within the ES. At culture days 7, 13, and 19, 4 mm punch biopsies were removed ($n=6$ per group and $n=6$ per time point) and immediately assessed following a protocol previously described.[53] Briefly, 0.5 mL of a sterile-filtered solution of 0.5 mg MTT/mL PBS was added to each well of a 24-well plate, containing one 4 mm punch. The biopsies were incubated in the MTT solution for 3 h at 37°C and 5% CO_2. After 3 h, the MTT solution was aspirated from the well, 0.5 mL methoxyethanol was added to each well (Fisher Scientific), and the solution was agitated on a rocking plate for 3 h to dissolve the formazan crystals. The amount of MTT-formazan product released was measured at 590 nm on a microplate reader with values reported as mean optical density ± standard deviation.

Surface electrical capacitance

Surface electrical capacitance (SEC) was performed to quantify the surface hydration of the ES. Surface hydration has been previously reported to be an accurate, reproducible method to nondestructively assess barrier function in skin where barrier function is inversely proportional to SEC. On culture days 7, 13, and 19, SEC measurements ($n=6$ per scaffold) were collected from the ES using a NOVA dermal phase meter (DPM 9003; NOVA Technology). Results are expressed as SEC ± standard deviation.

Immunohistochemistry

Biopsies were taken from the ES for histology at day 19. The biopsies were embedded in OCT resin and stored at −80°C until sectioning. For immunostaining, slides were fixed in methanol for 8 min, rehydrated in PBS, and incubated in primary antibodies for human involucrin (Molecular Probes) at 4°C overnight. The following day the sections were stained with the appropriate secondary antibody along with DAPI for 1 h at room temperature. Sections were rinsed with PBS, mounted with glycerin, and cover-slipped. The stained sections were imaged using an Olympus FV1000 Multi-Photon confocal microscope.

Statistical analysis

All data were analyzed using SigmaPlot 3.10 (Systat Software, Inc.). Differences between the groups were analyzed using One-Way ANOVA with a *post hoc* test of Tukey. Correlations were determined using the Pearson's correlation coefficient. p-values less than 0.05 were considered statistically significant.

Results

Physical and mechanical properties of acellular scaffolds

All electrospun scaffolds were comprised of continuous fibers with no beading or fiber bonding at the junctions (Fig. 1). Fibers within the coaxial and gelatin scaffolds

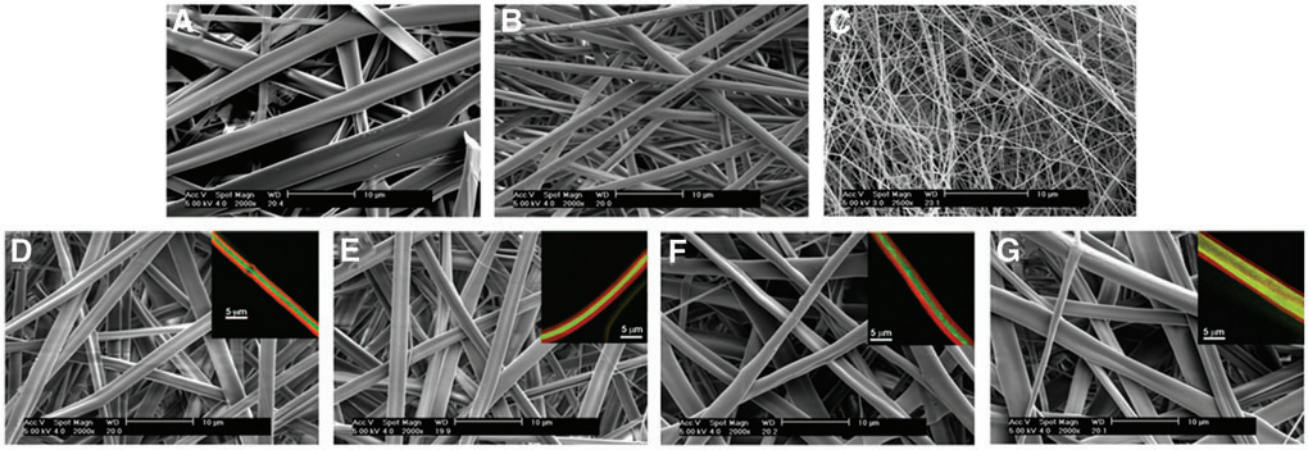

FIG. 1. Scanning electron micrographs of monofilament and coaxial scaffolds. Gelatin **(A),** polycaprolactone (PCL) **(B),** gelatin-PCL blend **(C),** CoA-S **(D),** CoA-M **(E),** CoA-L **(F),** CoA-XL **(G)**. Inset: confocal images of individual coaxial fibers showing gelatin (Red) and PCL (Green) Scale bar = 10 μm, Inset scale bar = 5 μm. Color images available online at www.liebertpub.com/tea

were more ribbon-like in morphology than the PCL or Blend (Fig. 1). In their as-spun condition, the gelatin and coaxial fibers appear to be similar in diameter and significantly smaller than PCL or the PCL-gelatin blend. Quantitative analysis of fiber diameter in the hydrated state revealed that the gelatin fibers were significantly larger than all other groups (Fig. 2). No significant difference in fiber diameter was found among the coaxial groups (Fig. 2). The thickness of the core in the coaxial fibers increased with solution concentration and flow rate (Fig. 2). Using confocal analysis, the core of the coaxial fibers was shown to be continuous with no observable mixing between the shell and core (Fig. 1D–G, inset). As expected, ATR-FTIR analysis of PCL showed strong peaks at 1724 cm^{-1} (carbonyl) and 1157–1240 corresponding to stretching of COC, OC-O, C-C, and C-O bonds (Fig. 3). The PCL samples had little background and greater absorbance than all other samples. The gelatin sample showed characteristic peaks at 1650 and 1540 cm^{-1} corresponding to amide bonds (Fig. 3). Characteristic peaks for PCL and gelatin were both seen in the blend samples, however, the intensity of these peaks were dampened. For the coaxial samples, the height of the amide bond peaks decreased as the shell thickness decreased (i.e., going from CoA-S to CoA-XL; Fig. 3). Characteristic PCL peaks were observed in all coaxial samples with no significant change in peak height (Fig. 3).

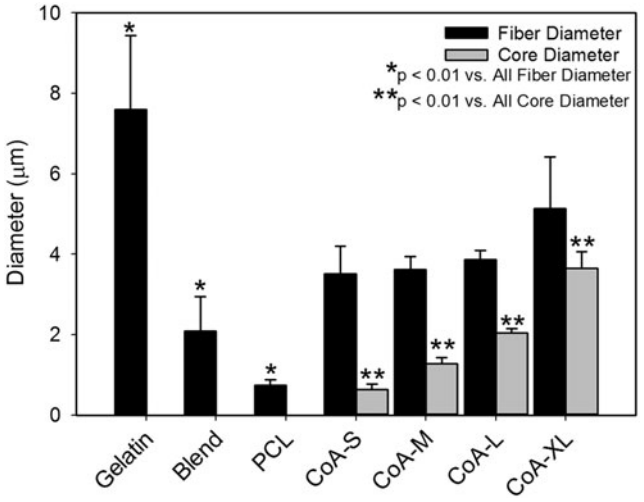

FIG. 2. Total fiber diameter and core diameter of hydrated scaffolds.

The mechanical properties of the gelatin scaffold were significantly lower than all other scaffolds while the PCL was stronger and stiffer than all other scaffolds ($p < 0001$). With the addition of a thin, submicron PCL core within the gelatin fibers, mechanical properties of the scaffold were significantly enhanced (Fig. 4). From no core (gelatin) to a ~3.65 μm diameter core (CoA-XL), the strength increased over 5.5-fold and stiffness increased over 25-fold (Fig. 4). The Blend was stronger than CoA-S and CoA-M but less stiff than CoA-L and CoA-XL (Fig. 4). Both UTS and linear stiffness scaled positively with increasing core diameter (CoA-S to CoA-XL).

Cell adhesion

The percent of fibroblasts and keratinocytes remaining after shear exposure was significantly decreased for cells on PCL and Blend scaffolds (Fig. 5A, B). There was no statistical difference in adhesion between gelatin and the coaxial scaffolds for both fibroblasts and keratinocytes.

ES viability, differentiation, and organization

Cellular metabolism on the pure PCL scaffold was significantly lower than all other scaffolds at all time points with the exception of the blend scaffold on day 7 (Fig. 6A). Coaxial scaffolds maintained cellular metabolism at a level equivalent to the pure gelatin scaffold for 13 days followed by a slight reduction in the CoA-XL group at day 19 (Fig. 6A).

To assess epidermal differentiation and barrier formation, surface hydration was measured using electrical capacitance (SEC). At culture day 7, ES was moist with no statistically significant difference among the groups (Fig. 6B). By day 13, no statistically significant differences between the ES grown on coaxial and gelatin scaffolds was observed and all were significantly decreased from blend and PCL samples.

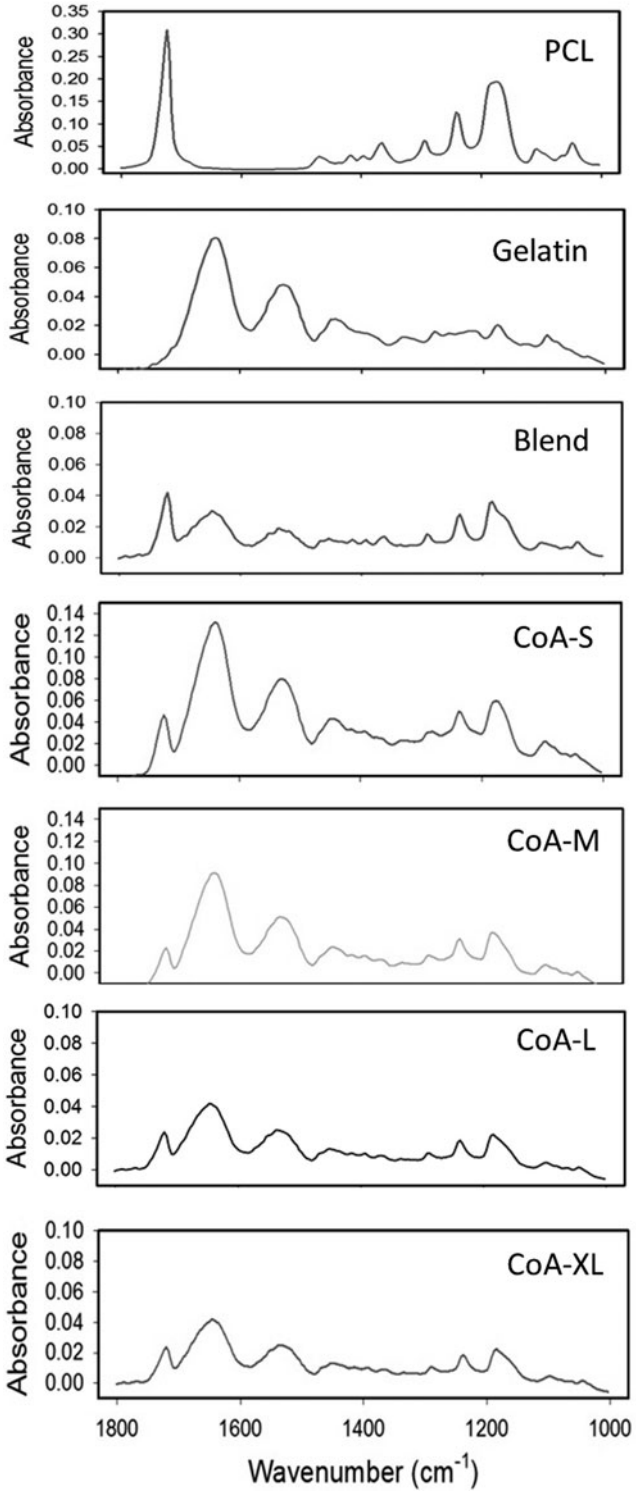

FIG. 3. Attenuated Total Reflectance-Fourier Transform Infrared (ATR-FTIR) spectroscopy of all scaffold types.

There was again no statistical difference between gelatin and coaxial scaffold samples at day 19, however, the CoA-M sample was not significantly different from the blend sample (Fig. 6B).

At day 19, all ES groups were embedded, cryosectioned, and stained with DAPI and involucrin to assess cellular organization and differentiation. ES formed using gelatin, blend, and coaxial electrospun scaffolds were well populated by fibroblasts (Fig. 7A, C–G). In contrast, fibroblasts were sparse in the PCL scaffold (Fig. 7B). Stratification of the dermal and epidermal layers was observed in the gelatin and coaxial scaffolds (Fig. 7A, D–G). However, epidermal and dermal layers appeared to be intermixing in Blend and PCL scaffolds with a poorly defined dermal–epidermal junction (Fig. 7B, C). The basal layer of epidermal keratinocytes, which is responsible for maintaining the epidermis, was not present in ES from the Blend and PCL scaffolds (Fig. 7B, C). Positive staining for involucrin, a suprabasal marker of epidermal differentiation, was observed in all coaxial and gelatin samples (Fig. 7A, D–G).

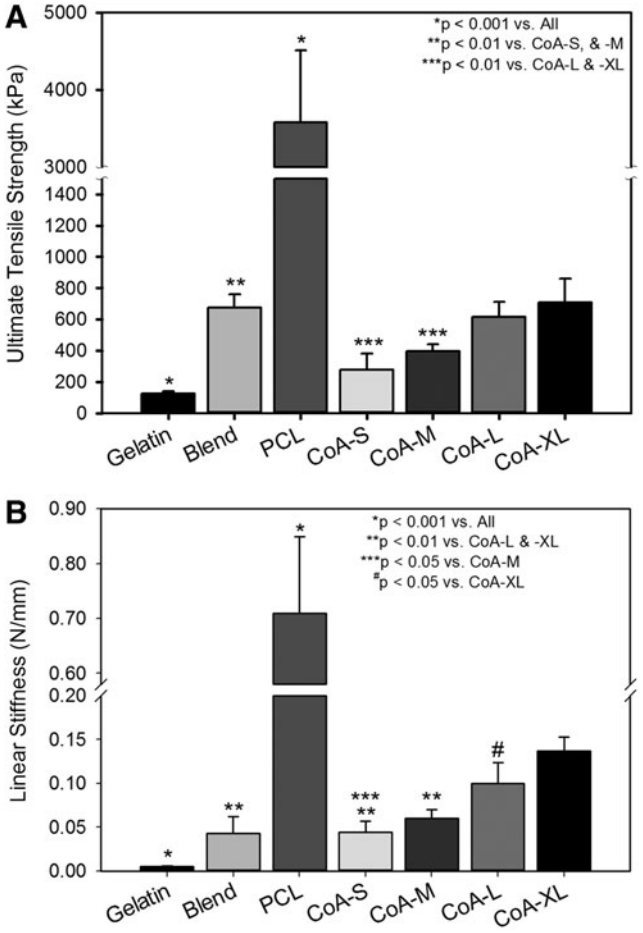

FIG. 4. Ultimate tensile strength (UTS) **(A)** and linear stiffness **(B)** of acellular scaffolds.

Mechanical properties of ES

The strength and stiffness of ES was greatest on PCL (Fig. 8A, B); however, the strength of ES fabricated with PCL was lower than that of the acellular PCL scaffold (3582.8 ± 931.3 kPa vs. 1445.5 ± 481.7 kPa, respectively) with no statistical difference in stiffness (0.7 ± 0.1 N/mm vs. 0.9 ± 0.4 N/mm, respectively). The addition of a PCL core to the gelatin fibers increased average ES strength and stiffness versus gelatin alone with significant improvements in CoA-M, -L, and–XL (Fig. 8A, B). Additionally, strength and stiffness of both the acellular scaffolds and ES correlated linearly with coaxial core diameter (Fig. 8C, D).

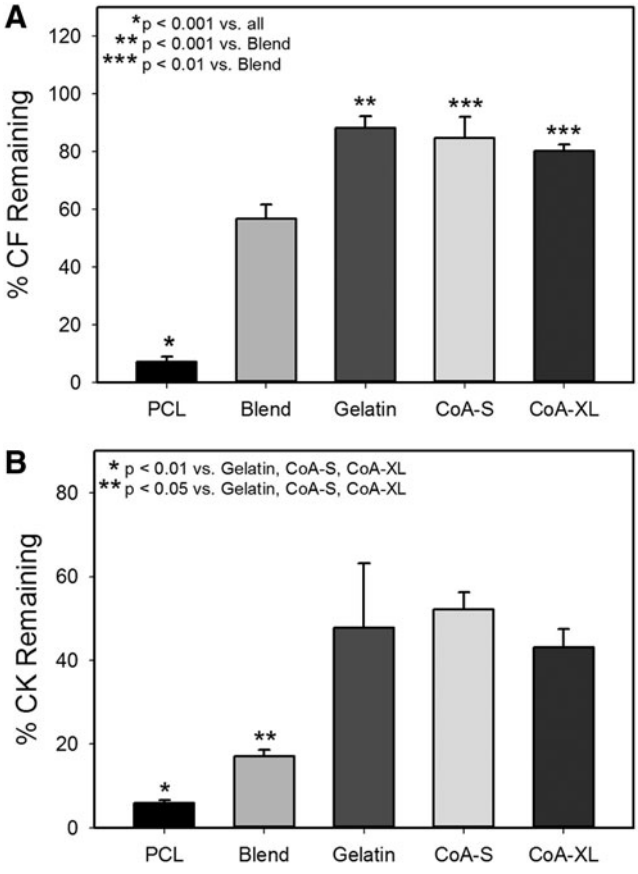

FIG. 5. Percent of fibroblasts **(A)** and keratinocytes **(B)** remaining on monofilament and coaxial fibers after exposure to 500 dynes/cm^2 of shear stress for 5 min. CK, epidermal keratinocytes; CF, dermal fibroblasts.

Discussion

The mechanical properties of ES are important to prevent graft damage *in vitro* and *in vivo* and to promote the greatest level of function after engraftment. As the mechanics of the dermal component of ES are dramatically lower than that of native human dermis,[26–30] targeting the scaffold component for biomechanical enhancement is a logical choice for improvement of whole ES mechanics. A major drawback to prior attempts to control the mechanics of ES via scaffold mechanics was that the alterations to the scaffold did not facilitate proper cell adhesion and tissue development due to either the toxicity of cross-linking agents[33] or poor adhesion and cell viability on synthetic polymers.[18] The advantage of coaxial electrospinning is that the shell provides a continuous biopolymer (i.e., gelatin) surface for cell interaction and prevents the cells from interacting with the PCL core. This system of shielding PCL with gelatin was shown to improve initial fibroblast and keratinocyte adhesion strength when compared with PCL or a PCL-gelatin blend (Fig. 4). Other studies have demonstrated the ability coaxial electrospun scaffolds have to support cellular adhesion and proliferation. These studies found proliferation[54,55] and adhesion[55] to be improved on coaxial scaffolds when compared with a 100% synthetic polymer scaffold and proliferation on a collagen/PCL coaxial scaffold was better than a collagen-coated PCL scaffold and not significantly different than a 100% collagen scaffold.[46]

The use of core diameter to tune the mechanical properties of the scaffold provides a platform for engineered tissue development where mechanics can be altered without any change to surface chemistry or scaffold architecture. No significant difference in overall structure was observed among the coaxial scaffolds with no change in total fiber diameter. FTIR showed that there is a distinct difference in chemistry between coaxial and blended scaffolds. As the depth of penetration for this technique is $\sim 2\,\mu m$, information from both the core and shell are observed in all coaxial scaffold, however, the intensity of the gelatin peaks scales positively with gelatin shell thickness. As the core diameter of the fiber increased, the UTS and stiffness of the scaffold increased likely due to a simple increase in total fraction of the high strength PCL within each fiber. This relationship between core diameter and coaxial scaffold mechanics follows a prior study by our lab that showed a linear relationship between core diameter and scaffold strength and stiffness in a highly cross-linked system.[40]

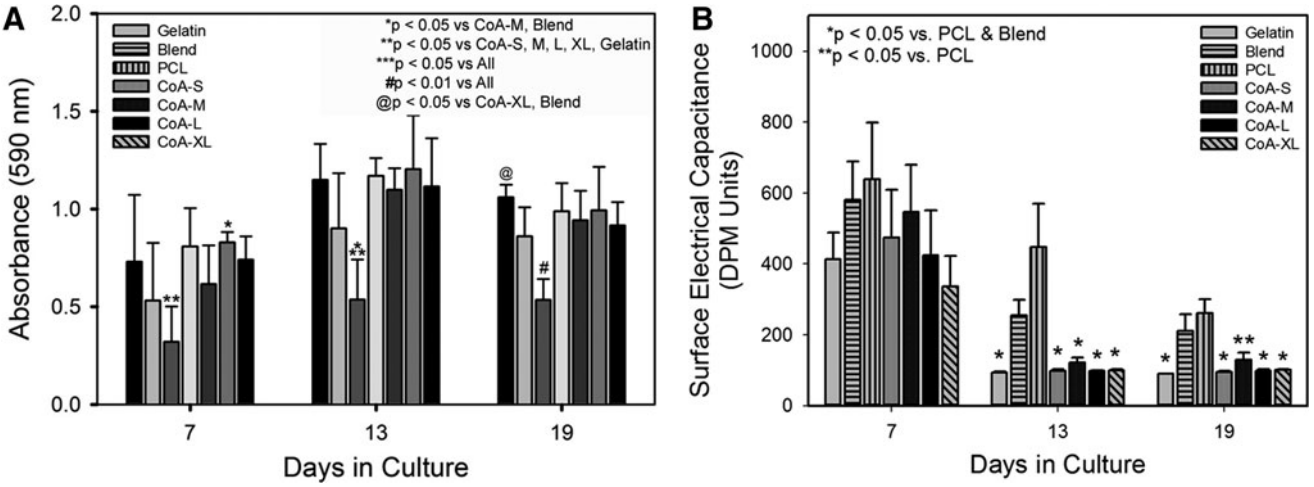

FIG. 6. MTT assay of cell metabolism in engineered skin as a function of scaffold type and time in culture **(A)**. Surface hydration measurements of engineered skin at days 7, 13, and 19 **(B)**. Note the significant reduction in hydration in the gelatin and coaxial groups by day 13.

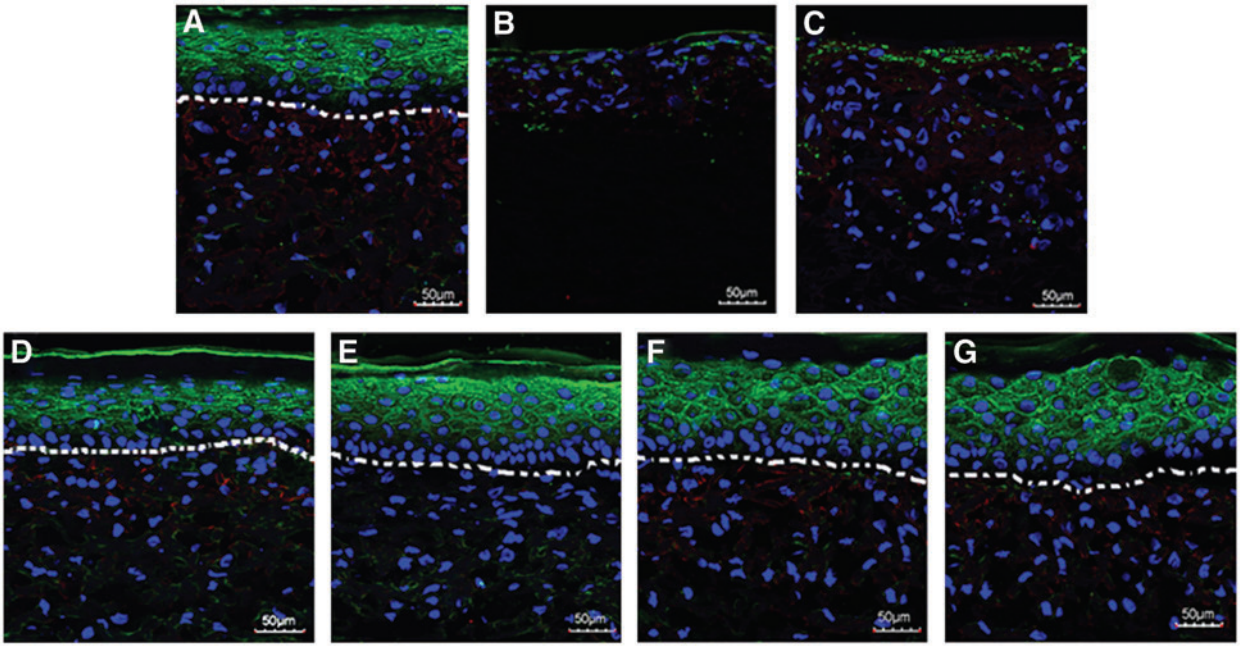

FIG. 7. Confocal images of engineered skin fabricated using gelatin **(A),** PCL **(B),** gelatin-PCL blend **(C),** CoA-S **(D),** CoA-M **(E),** CoA-L **(F),** CoA-XL **(G)** scaffolds at culture day 19. Nuclei are stained with DAPI (Blue) and the suprabasal epidermis with involucrin (Green). Dermal-epidermal junction outlined with dashed white line. Scale bar = 50 μm. Color images available online at www.liebertpub.com/tea

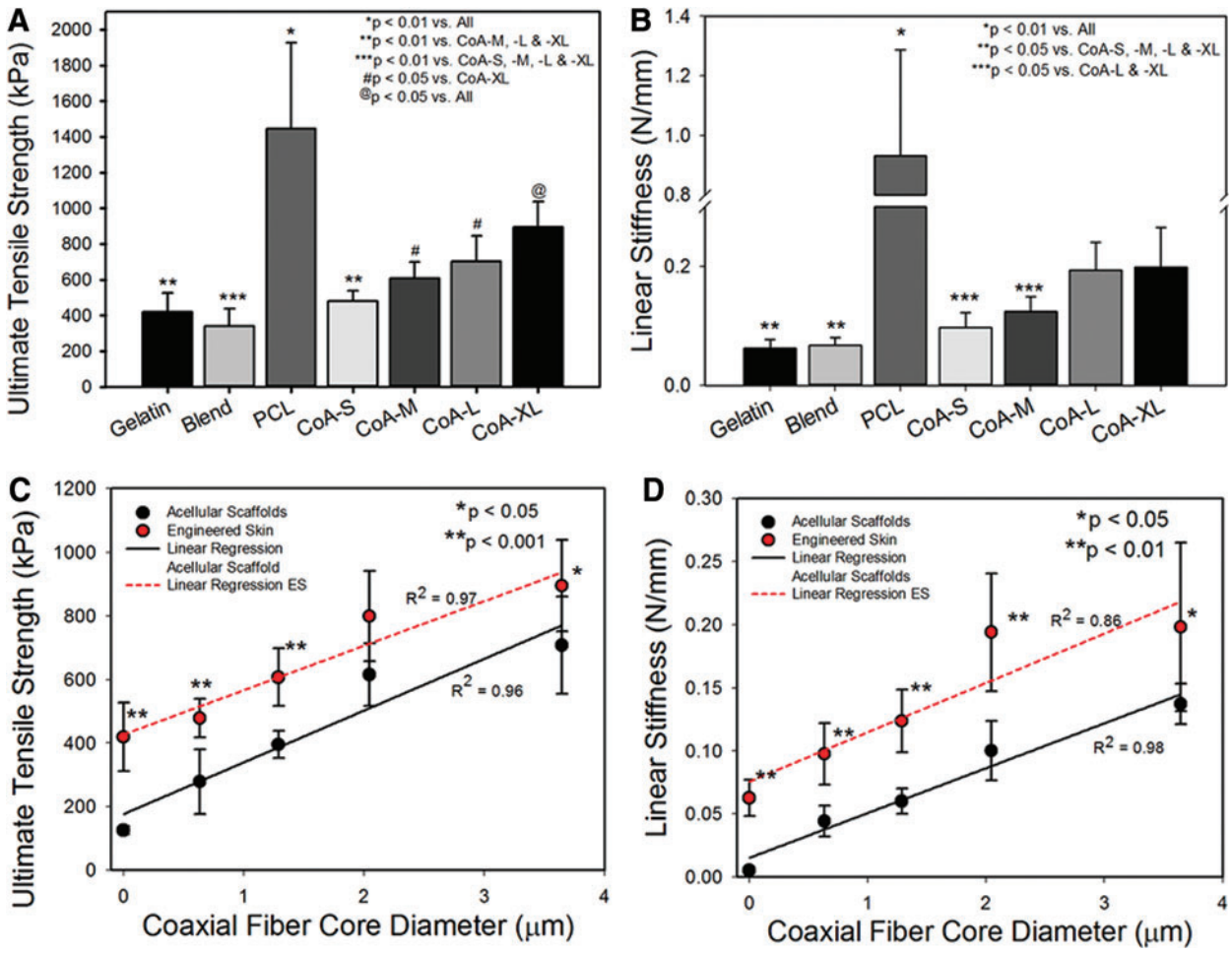

FIG. 8. UTS **(A)** and linear stiffness **(B)** of engineered skin fabricated with monofilament and coaxial scaffolds after 19 days in culture. Strength **(C)** and stiffness **(D)** of acellular scaffolds and engineered skin as a function of core diameter. Color images available online at www.liebertpub.com/tea

The ultimate goal of the study was to provide ES with tunable mechanics and thus the ability of these scaffolds to support cell viability and skin development is critical for the clinical function of these grafts. Growth of skin on electrospun gelatin was utilized as the positive control as skin cells have been shown to grow best on a 100% protein scaffold when compared with synthetic scaffolds[56] and electrospun gelatin scaffolds have previously been shown to support ES development.[57] All scaffolds were capable of promoting cellular attachment and growth; however, significantly lower cellular metabolism was observed in the PCL scaffold at all time points compared with ES fabricated with gelatin or coaxial scaffolds. Coaxial scaffolds supported cellular metabolism at the same level as the gelatin scaffold at all time points with the exception of day 19 where a slight reduction in metabolism was seen on CoA-XL. It is possible that the thinner gelatin shell in the CoA-XL scaffold may have led to a more rapid degradation of the shell and exposure of the PCL core in some areas of the scaffold, lowering cell adhesion and viability in that region. Lower cellular affinity has been previously reported on synthetic scaffolds when compared with natural polymer scaffolds.[55,56,58] Despite the small decrease in cellular activity on the CoA-XL scaffold versus the gelatin scaffold, the scaffold was shown to form a well-stratified ES graft.

Epidermal differentiation followed a similar trend as the viability measurements with the gelatin, CoA-S, CoA-M, CoA-L, and CoA-XL ES values of SEC approximating that of normal human skin (150–300 DPM) by day 13. At days 13 and 19, the blend and PCL groups were considerably wetter (i.e., higher SEC values and poor epidermal barrier function) than CoA and gelatin groups at days 13 and 19. Immunostaining for markers of epidermal differentiation (involucrin) also showed that the epidermis was poorly formed on PCL and blend scaffolds with no clear stratification of the epidermis and dermis. In the gelatin and CoA ES, a well-formed epidermis was seen with positive staining for the suprabasal layer of the epidermis. The increase in SEC values and malformed epidermis observed in both the PCL and the PCL-gelatin blend ES has been observed in similar studies of ES and has been attributed to deficiencies in culture conditions that prevent the formation of a stable epidermis.[18] The development of the epidermis relies on the formation of fibroblast dense dermis to support keratinocyte attachment. As it was shown that fibroblasts adhere more weakly to the PCL and blend, it is possible that a fraction of cells did not initially adhere to the scaffold and lead to the sparsely populated dermal layer seen in the ES.

UTS and linear stiffness of ES correlated linearly with increasing core diameter following a similar trend line as the acellular scaffolds. The addition of cells to the scaffold followed by 19 days of maturation added ~ 200 kPa to the failure strength of each construct indicating that extracellular matrix deposition and epidermal differentiation was equivalent on the gelatin and coaxial scaffolds. In contrast, ES fabricated with PCL showed a reduction in failure strength when compared with the acellular scaffold likely due to a combination of scaffold degradation and poor epidermal differentiation. Structural proteins, including involucrin and loricrin, are produced as skin matures, imparting biomechanical strength to the epidermis.[59,60] The absence of these proteins in a less differentiated epidermis was shown to increase the susceptibility of murine skin to damage.[61,62] Additionally, the sparse population of fibroblasts in the dermis of the PCL and blend ES would lead to relatively low levels of collagen and other matrix protein deposition when compared with gelatin and CoA ES.

The use of core diameter to control scaffolds mechanics and ES mechanics represents a technology platform that can be easily used to develop tissues with tunable mechanics. While the results of this study are promising, limitations to the present study involve the use of PCL as the core material. ES mechanics scaled positively with core diameter; however, overall ES mechanics remained low compared with normal human skin. Though it is not assumed that a direct match of mechanical properties between ES and native human skin is needed to significantly reduce graft damage during fabrication, shipping, and the early engraftment phase, reaching values within one to two orders of magnitude is hypothesized to facilitate ease of handling and the development of more robust skin mechanics *in vivo*. As the strength and stiffness of PCL are in the low range of mechanical properties of common biodegradable polymers used for biomedical applications,[63] the level of strength and stiffness we are able to attain is limited. Prior studies have shown that the use of a polyethersulfone core can increase the modulus of electrospun scaffolds greater than four-fold when compared with PCL alone.[64] Thus, the use of higher strength core materials may assist in reaching values closer to normal human skin. Although additional work is needed to assess how *in vitro* biomechanical improvements translate into *in vivo* mechanics following ECM remodeling, the platform proposed currently increased *in vitro* mechanics in a tunable manner improving handlability and eliminating damage during *in vitro* fabrication.

Conclusions

The poor mechanical properties of the current generations of ES lead to difficulties in surgical application and damage during fabrication and in the early phases of engraftment. Additionally, no strategies were previously available to tune ES biomechanics to match the native biomechanics at different anatomic locations. The current study showed that core diameter of PCL-gelatin coaxial scaffold facilitates the tuning of mechanical properties in ES with no deleterious effect on skin organization or function. This scaffold platform could be utilized not only to improve ease of manufacture and use but may also result in improved mechanical functionality post engraftment.

Acknowledgments

This work was partially supported by the National Science Foundation under Grant No. EEC-0914790, the Shriners Research Foundation (Grant #85100), and the Institute for Materials Research at The Ohio State University (Facilities Research Grant). The authors also thank the Campus Microscopy and Imaging Facility for confocal microscopy and the Center for Electron Microscopy and Analysis for scanning electron microscopy.

Disclosure Statement

No competing financial interests exist.

References

1. American Burn Association. National Burn Repository, www.ameriburn.org, 2012 (Accessed April 15, 2013).
2. Ressner, R.A., Murray, C.K., Griffith, M.E., Rasnake, M.S., Hospenthal, D.R., and Wolf, S.E. Outcomes of bacteremia in burn patients involved in combat operations overseas. J Am Coll Surgeons **206,** 439, 2008.
3. Rose, J., and Herndon, D. Advances in the treatment of burn patients. Burns **23,** S19, 1997.
4. Herndon, D.N., Barrow, R.E., Rutan, R.L., Rutan, T.C., Desai, M.H., and Abston, S. A comparison of conservative versus early excision. Therapies in severely burned patients. Ann Surg **209,** 547, 1989.
5. Fratianne, R., and Brandt, C. Improved survival of adults with extensive burns. J Burn Care Rehabil **18,** 347, 1997.
6. Sheridan, R.L., Remensnyder, J.P., Schnitzer, J.J., Schulz, J.T., Ryan, C.M., and Tompkins, R.G. Current expectations for survival in pediatric burns. Arch Pediatr Adolesc Med **154,** 245, 2000.
7. Gomez, M., Cartotto, R., Knighton, J., Smith, K., and Fish, J.S. Improved Survival Following Thermal Injury in Adult Patients Treated at a Regional Burn Center. J Burn Care Res **29,** 130, 2008.
8. Rafla, K., and Tredget, E.E. Infection control in the burn unit. Burns **37,** 5, 2011.
9. Berthod, F., and Damour, O. *In vitro* reconstructed skin models for wound coverage in deep burns. Br J Dermatol **136,** 809, 1997.
10. Michael, S., Sorg, H., Peck, C.T., Koch, L., Deiwick, A., Chichkov, B., *et al.* Tissue engineered skin substitutes created by laser-assisted bioprinting form skin-like structures in the dorsal skin fold chamber in mice. PLoS One **8,** e55741, 2013.
11. Hartmann-Fritsch, F., Hosper, N., Luginbühl, J., Biedermann, T., Reichmann, E., and Meuli, M. Human amniotic fluid derived cells can competently substitute dermal fibroblasts in a tissue-engineered dermo-epidermal skin analog. Pediart Surg Int **29,** 61, 2013.
12. Clement, A.L., Moutinho, T.J., and Pins, G.D. Micropatterned dermal–epidermal regeneration matrices create functional niches that enhance epidermal morphogenesis. Acta Biomater **9,** 9474, 2013.
13. Lagus, H., Sarlomo-Rikala, M., Bohling, T., and Vuola, J. Prospective study on burns treated with Integra®, a cellulose sponge and split thickness skin graft: comparative clinical and histological study-Randomized controlled trial. Burns **39,** 1577, 2013.
14. Huang, S., Xu, Y., Wu, C., Sha, D., and Fu, X. *In vitro* constitution and *in vivo* implantation of engineered skin constructs with sweat glands. Biomaterials **31,** 5520, 2010.
15. Lu, W., Yu, J., Zhang, Y., Ji, K., Zhou, Y., Li, Y., *et al.* Mixture of fibroblasts and adipose tissue-derived stem cells can improve epidermal morphogenesis of tissue-engineered skin. Cells Tissues Organs **195,** 197, 2012.
16. Biedermann, T., Klar, A.S., Böttcher-Haberzeth, S., Schiestl, C., Reichmann, E., and Meuli, M. Tissue-engineered dermo-epidermal skin analogs exhibit *de novo* formation of a near natural neurovascular link 10 weeks after transplantation. Pediatr Surg Int **30,** 165, 2014.
17. Haijian, L., Chu, Y., Zhang, Z., Zhang, G., Jiang, L., Wu, H., *et al.* Construction of bilayered tissue-engineered skin with human amniotic mesenchymal cells and human amniotic epithelial cells. Artif Organs **36,** 911, 2012.
18. Powell, H.M., and Boyce, S.T. Engineered human skin fabricated using electrospun collagen-PCL blends: morphogenesis and mechanical properties. Tissue Eng Part A **15,** 2177, 2009.
19. Sriwiriyanont, P., Lynch, K.A., Maier, E.A., Hahn, J.M., Supp, D., and Boyce, S.T. Morphogenesis of chimeric hair follicles in engineered skin substitutes with human keratinocytes and murine dermal papilla cells. Exp Dermatol **21,** 783, 2012.
20. Boyce, S.T., Kagan, R.J., Greenhalgh, D.G., Warner, P., Yakuboff, K.P., Palmieri, T., *et al.* Cultured skin substitutes reduce requirements for harvesting of skin autograft for closure of excised, full-thickness burns. J Trauma **60253,** 821, 2006.
21. Agache, P.G., Monneur, C., Leveque, J.L., and DeRigal, J. Mechanical properties and Young's modulus of human skin *in vivo*. Arch Dermatol Res **269,** 221, 1980.
22. Diridilluo, S., Vabre, V., Berson, M., Vaillant, L., Black, D., Lagarde, J.M., *et al.* Skin ageing: changes of physical properties of human skin *in vivo*. Int J Cosmetic Sci **23,** 353, 2001.
23. Wolff, E.F., Narayan, D., and Taylor, H.S. Long-term effects of hormone therapy on skin rigidity and wrinkles. Fertil Steril **82,** 285, 2005.
24. Cua, A.B., Wilhelm, K.P., and Maibach, H.I. Elastic properties of human skin: relation to age, sex, and anatomical region. Arch Dermatol Res **282,** 283, 1990.
25. Kuwahara, Y., Shima, Y., Shirayama, D., Kawai, M., Hagihara, K., Hirano, T., *et al.* Quantification of hardness, elasticity and viscosity of the skin of patients with systemic sclerosis using a novel sensing device (Vesmeter): a proposal for a new outcome measurement procedure. Rheumatology **47,** 1018, 2008.
26. Ebersole, G.C., Anderson, P.M., and Powell, H.M. Epidermal differentiation governs engineered skin biomechanics. J Biomech **43,** 3183, 2010.
27. LaFrance, H., Yahia, L., Germain, L., Guillot, M., and Auger, F.A. Study of the tensile properties of living skin equivalents. Bio-med Mater Eng **5,** 195, 1995.
28. Reihsner, R., and Menzel, E.J. On the orthogonal anisotropy of human skin as a function of anatomical region. Connect Tissue Res **34,** 145, 1996.
29. Jacquemoud, C., Bruyere-Garnier, K., and Coret, M. Methodology to determine failure characteristics of planar soft tissues using a dynamic tensile test. J Biomech **40,** 468, 2007.
30. Silver, F.H., Freeman, J.W., and DeVore, D. Viscoelastic properties of human skin and processed dermis. Skin Res Technol **7,** 18, 2001.
31. Powell, H.M., McFarland, K.L., Butler, D.L., Supp, D.M., and Boyce, S.T. Uniaxial strain regulates gene expression, morphogenesis and tissue strength in engineered skin. Tissue Eng Part A **16,** 1083, 2010.
32. Powell, H.M., and Boyce, S.T. Wound closure with EDC cross-linked cultured skin substitutes grafted to athymic mice. Biomaterials **28,** 1084, 2007.
33. Powell, H.M., and Boyce, S.T. EDC cross-linking improves skin substitute strength and stability. Biomaterials **27,** 5821, 2006.
34. Harrison, C.A., Gossiel, F., Layton, C.M., Bullock, A.J., Johnson, T., Blumsohn, A., *et al.* Use of an *in vitro* model of tissue-engineered skin to investigate the mechanism of skin graft contraction. Tissue Eng **12,** 3119, 2006.
35. Zhang, K., Qian, Y., Wang, H., Fan, L., Huang, C., Yin, A., *et al.* Genipin-crosslinked silk fibroin/hydroxybutyl chitosan nanofibrous scaffolds for tissue-engineering application. J Biomed Mater Res A **95A,** 870, 2010.

36. Shalumon, K.T., Sathish, D., Nair, S.V., Chennazhi, K.P., Tamura, H., and Jayakumar, R. Fabrication of aligned poly(lactic acid)-chitosan nanofibers by novel parallel blade collector method for skin tissue engineering. J Biomed Nanotechnol **8,** 405, 2012.
37. Asran, A.S., Razghandi, K., Aggarwal, N., Michler, G.H., and Groth, T. Nanofibers from blends of polyvinyl alcohol and polyhydroxy butyrate as potential scaffold material for tissue engineering of skin. Biomacromolecules **11,** 3413, 2010.
38. Chandrasekaran, A.R., Venugopal, J., Sundarrajan, S., and Ramakrishna, S. Fabrication of a nanofibrous scaffold with improved bioactivity for culture of human dermal fibroblasts for skin regeneration. Biomed Mater **6,** 015001, 2011.
39. Zhou, Y., Yang, D., Chen, X., Xu, Q., Lu, F., and Nie, J. Electrospun water-soluble carboxyethyl chitosan/poly(vinyl alcohol) nanofibrous membrane as potential wound dressing for skin regeneration. Biomacromolecules **9,** 349, 2008.
40. Drexler, J.W., and Powell, H.M. Regulation of electrospun scaffold stiffness via coaxial core diameter. Acta Biomater **7,** 1133, 2011.
41. Han, D., Boyce, S.T., and Steckl, A.J. Versatile core-sheath biofibers using coaxial electrospinning. Mater Res Soc **1094,** 1, 2008.
42. Dhandayuthapani, B., Krishnan, U.M., and Sethuraman, S. Fabrication and characterization of chitosan-gelatin blend nanofibers for skin tissue engineering. J Biomater Appl **94B,** 264, 2010.
43. Rahman, M.M., Pervez, S., Nesa, B., and Khan, M.A. Preparation and characterization of porous scaffold composite films by blending chitosan and gelatin solutions for skin tissue engineering. Polym Int **62,** 79, 2013.
44. Vatankhah, E., Prabhakaran, M.P., Jin, G., Mobarakeh, L.G., and Ramakrishna, S. Development of nanofibrous cellulose acetate/gelatin skin substitutes for variety wound treatment applications. J Biomater Appl **28,** 909, 2014.
45. Ng, K.W., Hutmacher, D.W., Schantz, J.T., Seng, C., Too, H.P., Lim, T.C., *et al.* Evaluation of ultra-thin poly(ε-caprolactone) films for tissue-engineered skin. Tissue Eng **7,** 441, 2001.
46. Zhang, Y.Z., Venugopal, J., Huang, Z.M., Lim, C.T., and Ramakrishna, S. Characterization of the surface biocompatibility of the electrospun PCL-collagen nanofibers using fibroblasts. Biomacromolecules **6,** 2583, 2005.
47. Duan, H., Feng, B., Guo, X., Wang, J., Zhou, G., *et al.* Engineering of epidermis skin grafts using electrospun nanofibrous gelatin/polycaprolactone membranes. Int J Nanomed **8,** 2077, 2013.
48. Gautam, S., Chou, C.F., Dinda, A.K., Potdar, P.D., and Mishra, N.C. Surface modification of nanofibrous polycaprolactone/gelatin composite scaffold by collagen type I grafting for skin tissue engineering. Mater Sci Eng C Mater Biol Appl **34,** 402, 2012.
49. Zhang, Y., Ouyang, H., Lim, C.T., Ramakrishna, S., and Huang, Z.M. Electrospinning of gelatin fibers and gelatin/PCL composite fibrous scaffolds. J Biomed Mater Res B **72B,** 156, 2005.
50. Chong, E.J., Phan, T.T., Lim, I.J., Zhang, Y.Z, Bay, B.H., Ramakrishna, S., *et al.* Evaluation of electrospun PCL/gelatin nanofibrous scaffold for wound healing and layered dermal reconstruction. Acta Biomater **3,** 321, 2007.
51. Blackstone, B.N., Willard, J.J., Lee, C.H., Nelson, M.T., Hart, R.T., Lannutti, J.J. *et al.* Plasma surface modification of electrospun fibers for adhesion-based cancer cell sorting. Integr Biol **4,** 1112, 2012.
52. Swope, V.B., Supp, A.P., Schwemberger, S., Babcock, G., and Boyce, S.T. Increased expression of integrins and decreased apoptosis correlate with increased melanocyte retention in cultured skin substitutes. Pigm Cell Res **19,** 424, 2006.
53. Mosmann, T. Rapid colorimetric assay for cellular growth and survival: application to proliferation and cytotoxicity assays. J Immunol Methods **65,** 55, 1983.
54. Zhao, P., Jiang, H., Pan, H., Zhu, K., and Chen, W. Biodegradable fibrous scaffolds composed of gelatin coated poly(ε-caprolactone) prepared by coaxial electrospinning. J Biomed Mater Res **83A,** 372, 2007.
55. Wu, L., Li, H., Li, S., Li, X., Yuan, X., Li, X. *et al.* Composite fibrous membranes of PLGA and chitosan prepared by coelectrospinning and coaxial electrospinning. J Biomed Mater Res **92A,** 563, 2010.
56. Venugopal, J.R., Zhang, Y., and Ramakrishna, S. *In vitro* culture of human dermal fibroblasts on electrospun polycaprolactone collagen nanofibrous membrane. Artif Organs **30,** 440, 2006.
57. Powell, H.M., and Boyce, S.T. Fiber density of electrospun gelatin scaffolds regulates morphogenesis of dermal–epidermal skin substitutes. J Biomed Mater Res A **84A,** 1078, 2008.
58. Thomson, R.C., Shung, A.K., Yaszemski, M.J., and Mikos, A.G. Polymer scaffold processing. In: Lanza, R.P., Langer, R., Vacanti, J., eds. Principles of Tissue Engineering. Second Edition. California: Elsevier Science, 2000, pp. 251–262.
59. Candi, E., Schmidt, R., and Melino, G. The cornified envelope: a model of cell death in the skin. Nat Rev Mol Cell Bio **6,** 328, 2005.
60. Nemes, Z., and Steinert, P.M. Bricks and mortar of the epidermal barrier. Exp Mol Med **31,** 5, 1999.
61. Koch, P.J., de Viragh, P.A., Scharer, E., Bundman, D., Longley, M.A., Bickenbach, J., *et al.* Lessons from loricrin-deficient mice: compensatory mechanisms maintaining skin barrier function in the absence of a major cornified envelope protein. J Cell Biol **151,** 389, 2000.
62. Ishida-Yamamoto, A., and Iizuka, H. Structural organization of cornified cell envelopes and alterations in inherited skin disorders. Exp Dermatol **7,** 1, 1998.
63. Engelberg, I., and Kohn, J. Physico-mechanical properties of degradable polymers used in medical applications: a comparative study. Biomaterials **12,** 292, 1991.
64. Nam, J., Johnson, J., Lannutti, J.J., and Agarwal, S. Modulation of embryonic mesenchymal progenitor cell differentiation via control over pure mechanical modulus in electrospun nanofibers. Acta Biomat **7,** 1516, 2011.

Address correspondence to:
Heather Megan Powell, PhD
Department of Biomedical Engineering
The Ohio State University
116 W. 19th Ave., 243C Fontana Labs
Columbus, OH 43210

E-mail: powell.299@osu.edu

Received: November 6, 2013
Accepted: April 2, 2014
Online Publication Date: May 19, 2014